

**Down-Conversion Mixers for 60-GHz
Wireless Communications Based on
Schottky Barrier Diodes Fabricated in
Standard CMOS Technology**

Minsu Ko

THE GRADUATE SCHOOL

YONSEI UNIVERSITY

Department of Electrical and Electronic Engineering

**Down-Conversion Mixers for 60-GHz
Wireless Communications Based on
Schottky Barrier Diodes Fabricated in
Standard CMOS Technology**

by

Minsu Ko

Submitted to the Department of Electrical and Electronic Engineering
and the Graduate School of Yonsei University in partial fulfillment of
the requirements for the degree of

Master of Science

at the

**THE GRADUATE SCHOOL
YONSEI UNIVERSITY**

January 2008

This certifies that the master's thesis of
Minsu Ko is approved.

Thesis Supervisor: Woo-Young Choi

Yongshik Lee

Tae Wook Kim

**THE GRADUATE SCHOOL
YONSEI UNIVERSITY**

January 2008

To my family and love

Table of Contents

TABLE OF CONTENTS	V
LIST OF FIGURES AND TABLES	VII
ABSTRACT	X
I. INTRODUCTION	1
I-1. WIRELESS COMMUNICATIONS AT 60 GHz	1
I-2. LOW-COST AND LOW-COMPLEXITY COMMUNICATIONS	3
I-3. SQUARE-LAW MIXERS AT RECEIVERS	5
I-4. OUTLINE OF DISSERTATION	6
II. SCHOTTKY BARRIER DIODES IN CMOS TECHNOLOGY	8
II-1. SCHOTTKY AND OHMIC CONTACTS IN SCHOTTKY BARRIER DIODES	8
II-2. FABRICATION OF SCHOTTKY BARRIER DIODES IN CMOS TECHNOLOGY	12

II-3. MODELING OF SCHOTTKY BARRIER DIODES	16
II-3-A. <i>DC Characterization of Schottky Barrier Diodes</i>	20
II-3-B. <i>RF Characterization of Schottky Barrier Diodes</i>	23
III. 60-GHZ SQUARE-LAW DOWN-CONVERSION MIXER.....	28
III-1. DESIGN OF 60-GHZ MIXER USING SCHOTTKY BARRIER DIODES	28
III-2. PASSIVE COMPONENTS FOR 60-GHZ MIXER	31
III-3. PERFORMANCE OF 60-GHZ MIXER	34
IV. 60-GHZ COMMUNICATION DEMONSTRATIONS USING FABRICATED MIXER	41
IV-1. PRINCIPLES OF SELF-HETERODYNE SYSTEMS.....	41
IV-2. BROADBAND DATA TRANSMISSION IN 60-GHZ SELF- HETERODYNE SYSTEM.....	43
IV-3. BROADBAND DATA TRANSMISSION IN 60-GHZ ASK SYSTEM..	49
V. SUMMARY	54
REFERENCES.....	57
국문요약.....	62

List of Figures and Tables

Figure I.1	Block diagram of 60-GHz RF transceiver for self-heterodyne systems and ASK systems.....	4
Figure I.2	Transmitter output spectrum of (a) self-heterodyne systems and (b) ASK systems.....	4
Figure II.1	Energy band diagrams for ideal metal-semiconductor contacts between a metal and an n-type semiconductor: $\Phi_M > \Phi_S$ system (a) an instant after contact formation and (b) under equilibrium conditions; $\Phi_M < \Phi_S$ system (c) an instant after contact formation and (d) under equilibrium conditions.....	10
Figure II.2	Surface potential-energy barriers and work functions of metal silicides in n-Si semiconductor	11
Figure II.3	Ohmic contact formation in heavily doped semiconductor	11
Figure II.4	SBD cell: (a) cross-sectional view (b) layout	14
Figure II.5	Layout of 25 SBD cells connected in parallel.....	15
Figure II.6	Equivalent circuit model of SBD.....	18
Figure II.7	Measurement setup for characterization of SBD.....	19
Figure II.8	Measured and fitted DC I-V curves of SBD.....	22
Figure II.9	Measured diode resistance and capacitance of fabricated SBD versus frequency (when diode voltage is zero).....	25

Figure II.10	Measured and fitted S-parameters of SBD (when diode voltage is 0.0, 0.2, 0.3, 0.4, and 0.5 V)	26
Table II.1	Extracted parameters of SBD	27
Figure III.1	Schematic of 60-GHz down-conversion mixer	30
Figure III.2	Chip photo of fabricated 60-GHz down-conversion mixer	30
Figure III.3	Characteristic impedance of $\lambda_{60GHz} / 4$, 50- Ω microstrip line	32
Figure III.4	Electrical length of $\lambda_{60GHz} / 4$, 50- Ω microstrip line.....	32
Figure III.5	Insertion loss of $\lambda_{60GHz} / 4$, 50- Ω microstrip line	33
Figure III.6	Frequency response of fabricated LPF	33
Figure III.7	Return loss of the mixer: (a) input and (b) output (when bias voltage is 1 V)	37
Figure III.8	Experimental setup for measurement of conversion loss of mixer.....	38
Figure III.9	IF mixer output power versus RF mixer input power (when LO power = RF power and RF frequency of 60.5 GHz)	38
Figure III.10	Conversion loss versus RF mixer input power (when LO power = RF power and RF frequency of 60.5 GHz)	39
Figure III.11	Conversion loss versus RF frequency (when RF (LO) mixer input power is -25 dBm).....	39
Table III.1	Performance summary of fabricated 60-GHz square-law down-conversion mixer and comparisons with pervious works.....	40

Figure IV.1	Experimental setup for 60-GHz self-heterodyne system	46
Figure IV.2	60-GHz transmitter output spectrum in self-heterodyne system with LO signal and BPSK-modulated RF signal	47
Figure IV.3	Received IF output spectra in self-heterodyne system: (a) without receiver IF BPF and (b) with receiver IF BPF	47
Figure IV.4	Relationship between IF output power and bit error rate for back-to-back link and 60-GHz self-heterodyne link	48
Figure IV.5	Experimental setup for 60-GHz ASK system	51
Figure IV.6	Spectra in 60-GHz ASK system: (a) transmitter output signal and (b) baseband output signal	52
Figure IV.7	BER versus total received signal power and calculated propagation distance for 60-GHz self-heterodyne system (Tx and Rx antenna gain of 24 dBi each)	53

Abstract

Self-heterodyne systems and ASK systems having the simple receiver architecture with square-law down-conversion mixers and robustness of local oscillator performance are proposed for low-complexity and low-cost 60-GHz wireless communication. For that, a 60-GHz square-law down-conversion mixer based on Schottky barrier diodes in the 0.18- μm CMOS technology is investigated. Fabricated Schottky barrier diodes have a cut-off frequency of 250 GHz, which is feasible for 60-GHz applications. And the equivalent circuit model of diodes is developed for use of circuit design. Passive components used by the mixer such as the transmission line and the low pass filter are also characterized. Based on these diodes, the 60-GHz square-law down-conversion mixer is implemented. The measured peak conversion loss is 23.7 dB when each RF and LO power is -3 dBm. At last, 622-Mb/s data transmission in the 60-GHz self-heterodyne system and the ASK system using the fabricated mixer is demonstrated. In the 60-GHz self-heterodyne system, the bit error rate is achieved below 10^{-10} with the propagation loss of 24 dB. In the 60-GHz ASK system, the bit error rate is achieved below 10^{-10} with the propagation loss of 22 dB.

I. Introduction

I-1. Wireless Communications at 60 GHz

Over the past decade, there has been significant progress in the development of wireless communication technologies. Recently, the demand of users is moving into higher capacity transmission such as high quality multimedia services, high speed internet access, and wireless data bus for cable replacement. For that, wireless systems using millimeter-wave bands can be a solution. Especially, communications using the 60-GHz band have been enthusiastically discussed and studied.

Form 2003, standardization of 60-GHz band millimeter-wave wireless personal area network (mmW WPAN) systems has been discussed in the IEEE 802.15 TG3c [1]. It uses the 57 ~ 66-GHz band and it supports data rate up to 3.5 Gb/s for the target application of wireless HDTV video transmission. The 60-GHz band provides enough bandwidth for gigabit data transmission, short-range and high-frequency-reuse transmission by high atmospheric absorption, and high directivity with small-size and high-gain antennas. Most of all, main attractiveness of 60 GHz is that the 60-GHz band is specified as a

license-free band in many countries [2].

With interests in 60 GHz, research results on low-cost 60-GHz RF transceivers have been reported by using 90-nm or 0.13- μm standard CMOS technologies [3], [4]. However, some challenges are remained to implement 60-GHz transceivers in standard CMOS technologies, which are design of high power amplifiers and frequency synthesizers having low phase noise under -90dBc/Hz at 1 MHz [5]. These burdens lead higher cost for use of high-performance fabrication technologies and slower time to market than market growth. For that, low-cost and low-complexity communication schemes such as self-heterodyne systems and amplitude-shift keying (ASK) systems can be alternatives.

I-2. Low-Cost and Low-Complexity Communications

Self-heterodyne systems and ASK systems enable simpler and more cost-effective RF transceivers. Two systems can be developed by same transceiver architecture as shown in Figure I.1. At first, in self-heterodyne systems, the transmitter transmits not only frequency up-converted RF signals but also a LO signal simultaneously as shown in Figure I.2 (a). And the receiver performs frequency down-conversion of these signals to IF band by using a square-law mixer. Through this scheme, configuration of the receiver can be simple without a local oscillator. Moreover, performance requirements of the local oscillator at the transmitter are relaxed because problems caused by phase noise and frequency offset at the transmitter are eliminated at the receiver [6]. A drawback is requiring large bandwidth for both RF and LO signals.

On the other hand, ASK systems can be thought as zero-IF self-heterodyne systems. ASK systems directly up-convert digital baseband data to RF as shown in Figure I.2 (b). Therefore, in addition to advantages of self-heterodyne systems, analog-to-digital conversion overhead is substantially reduced [7].

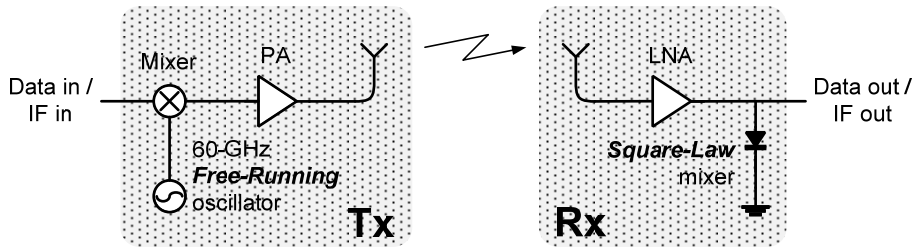


Figure I.1 Block diagram of 60-GHz RF transceiver for self-heterodyne systems and ASK systems

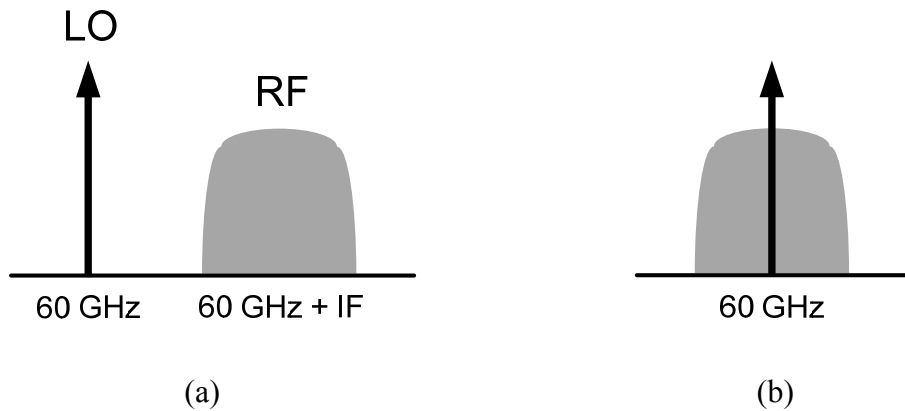


Figure I.2 Transmitter output spectrum of (a) self-heterodyne systems and (b) ASK systems

I-3. Square-Law Mixers at Receivers

The key component implementing self-heterodyne or ASK receivers is a square-law down-conversion mixer. In comparison with conventional mixers, it is not a three-terminal device, but a two-terminal device which has the RF/LO input port and the IF output port. The RF signal and the LO signal received from the transmitter are mixed by a square-law operation of the mixer. At the output port, the down-converted IF signal is represented by

$$\begin{aligned} v_{IF}(t) &= (v_{RF}(t) + v_{LO}(t))^2 && (1-1) \\ &= (V_{RF} \cos w_{RF}t + V_{LO} \cos w_{LO}t)^2 \\ &= V_{RF}V_{LO} \cos(w_{RF} - w_{LO})t + \dots \end{aligned}$$

Square-law mixers can be designed by a simple diode configuration. For operating mixers at 60 GHz, high-speed Schottky barrier diodes are considered. Fabrication of Schottky barrier diodes having a cut-off frequency of 400 GHz in the standard 0.18- μm CMOS technology was reported in [8]. Therefore, it is expected that down-conversion mixers for self-heterodyne receivers and ASK receivers can be simply designed by using SBDs fabricated in the low-cost standard 0.18- μm CMOS technology.

I-4. Outline of Dissertation

This dissertation will focus on 60-GHz down-conversion mixers based on Schottky barrier diodes (SBDs) fabricated in the standard CMOS technology, and their applications to 60-GHz ASK systems and self-heterodyne systems. At first, Fabrication, characterization, and modeling of SBDs will be explained, and then design of the 60-GHz square-law down-conversion mixer will be described. Finally, 60-GHz self-heterodyne system and ASK systems will be demonstrated for broadband data transmission by using the fabricated mixer. Details of dissertation outline are as follows.

In chapter II, SBDs fabricated in the standard CMOS technology are introduced. Section II-1 explains basic principles of SBDs in terms of Schottky contacts and ohmic contacts. In section II-2, the fabrication method of SBDs is presented with layouts of fabricated SBDs. In last section in this chapter, DC & RF characteristics and modeling results of SBDs fabricated in the standard 0.18- μm CMOS technology are shown, and equivalent circuit model parameters are also presented.

Next, in chapter III, the 60-GHz down-conversion mixer based on the square-law operation by using SBDs is described. At first, a design method of the mixer is explained in section III-1. And then, passive

components used for the mixer are described in section III-2. In section III-3, simulation performance and measured performance of the mixer are observed in terms of the input/output matching and the conversion loss versus the input power and RF frequencies.

In chapter IV, demonstration of broadband data transmission at 60 GHz is performed by using the fabricated mixer. In section IV-1, principles of self-heterodyne systems are introduced. In section IV-2, the 60-GHz self-heterodyne system is demonstrated with 1.4-GHz, 622-Mb/s binary phase-shift keying (BPSK) data. The 60-GHz ASK system is also demonstrated with 622-Mb/s non-return-to-zero (NRZ) data in section IV-3.

At last, chapter V summarizes results of SBDs, the 60-GHz down-conversion mixer fabricated in the standard 0.18- μm CMOS technology, and 60-GHz RF system demonstration. And future work is also explained.

II. Schottky Barrier Diodes in CMOS Technology

II-1. Schottky and Ohmic Contacts in Schottky Barrier Diodes

The Schottky barrier diode (SBD) is formed by metal-semiconductor contacts, which are the Schottky contact and the ohmic contact. These are characterized by Φ_M , Φ_S , and χ which are work functions of a metal and a semiconductor, and the electron affinity of the semiconductor. And the surface potential-energy barrier height, $\Phi_B = \Phi_M - \chi$, determines a type of contacts. As shown in Figure II.1, the Schottky contact is formed by the high barrier height, and the ohmic contact is formed by the low barrier height [9].

Practically, contacts in a diode are formed in same materials such as silicon, so the barrier height is not a controllable parameter. Therefore, a type of contacts cannot be chosen by the barrier height. Figure II.2 shows the barrier heights and the work functions of metals in a Si process with various metal silicides [10]. In CMOS technologies, TiSi_2 and CoSi_2 are commonly used for metal silicides, and their barrier heights have values of about 0.60 and 0.64.

To produce ohmic contacts in a high barrier condition, heavily

doping the surface region of the semiconductor is used. As shown in Figure II.3, a metal-semiconductor contact in lowly doped semiconductor produces a common Schottky contact. However, a contact in highly doped semiconductor forms very narrow barrier, hence even low energy majority carriers can transfer through the barrier via the tunneling process. Therefore, it effectively operates like an ohmic contact [9].

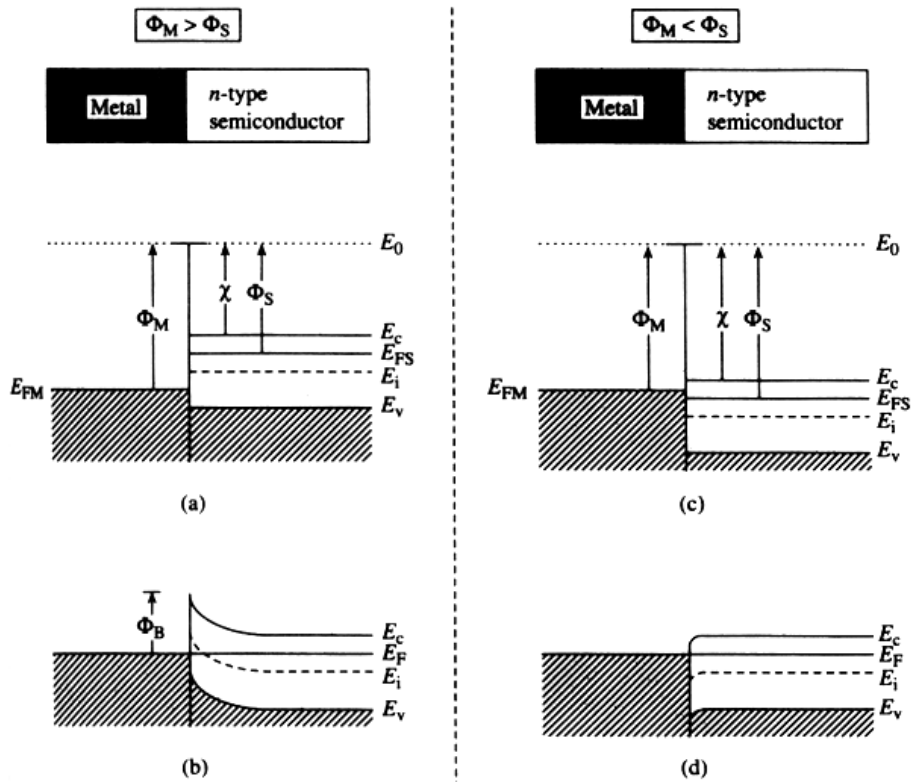


Figure II.1 Energy band diagrams for ideal metal-semiconductor contacts between a metal and an n-type semiconductor: $\Phi_M > \Phi_S$ system (a) an instant after contact formation and (b) under equilibrium conditions; $\Phi_M < \Phi_S$ system (c) an instant after contact formation and (d) under equilibrium conditions

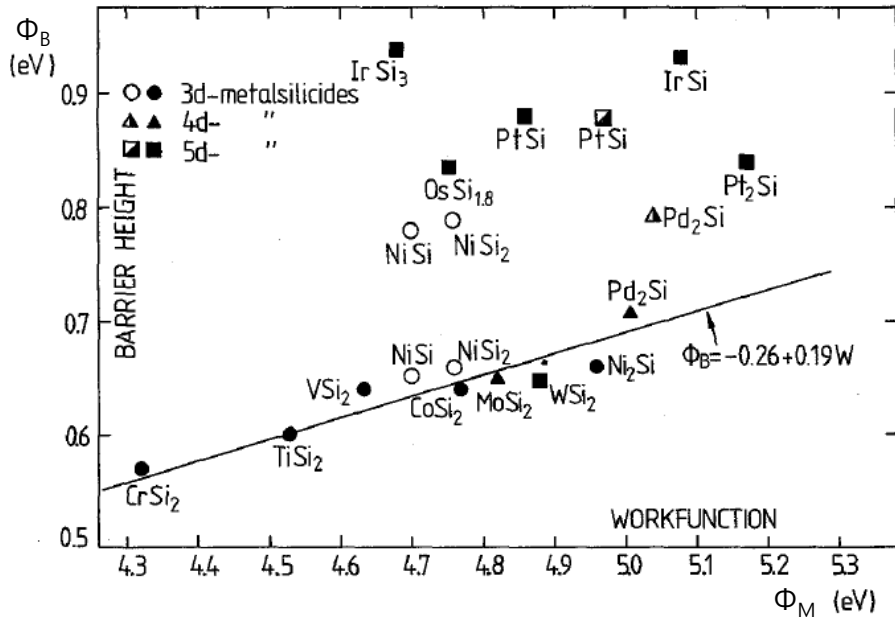


Figure II.2 Surface potential-energy barriers and work functions of metal silicides in n-Si semiconductor

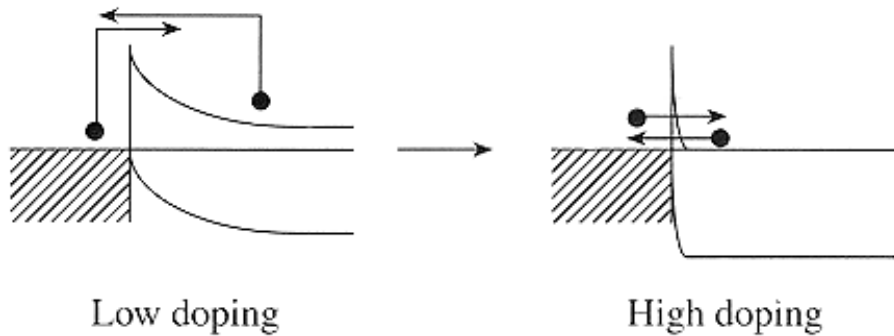


Figure II.3 Ohmic contact formation in heavily doped semiconductor

II-2. Fabrication of Schottky Barrier Diodes in CMOS Technology

To evaluate feasibility of the SBD as a 60-GHz device, the SBD cell was fabricated in the standard CMOS technology as shown in Figure II.4 [8]. The Schottky contact at the anode is formed between the cobalt metal salicide layer and the lowly doped n-well layer. The ohmic contact at the cathode is formed between the salicide layer and the highly doped n+ layer. For the one-port configuration, metal layer 1~6 are used at the anode to connect to the signal line of the metal 6. And the metal layer 1 is used at the cathode to connect to the ground plane of the metal 1.

To operate the SBD at 60 GHz, it should be designed carefully to achieve its cut-off frequency of 60 GHz above. The cut-off frequency of the SBD, f_c , is given by [11]

$$f_c = \frac{1}{2\pi RC} \quad (2-1)$$

where

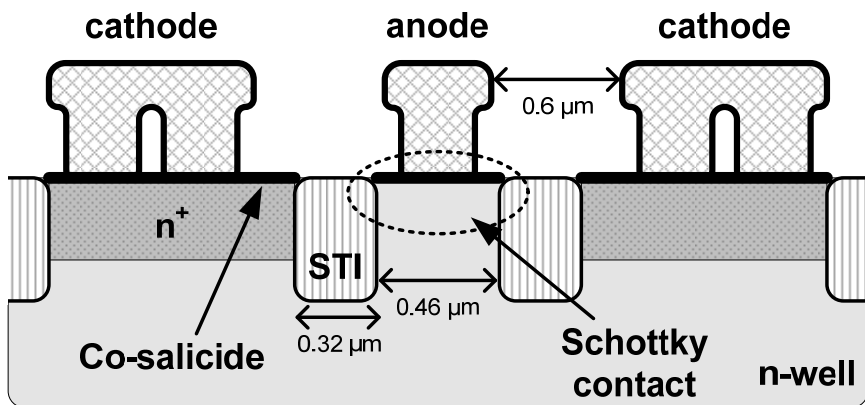
R diode on-resistance

C diode capacitance

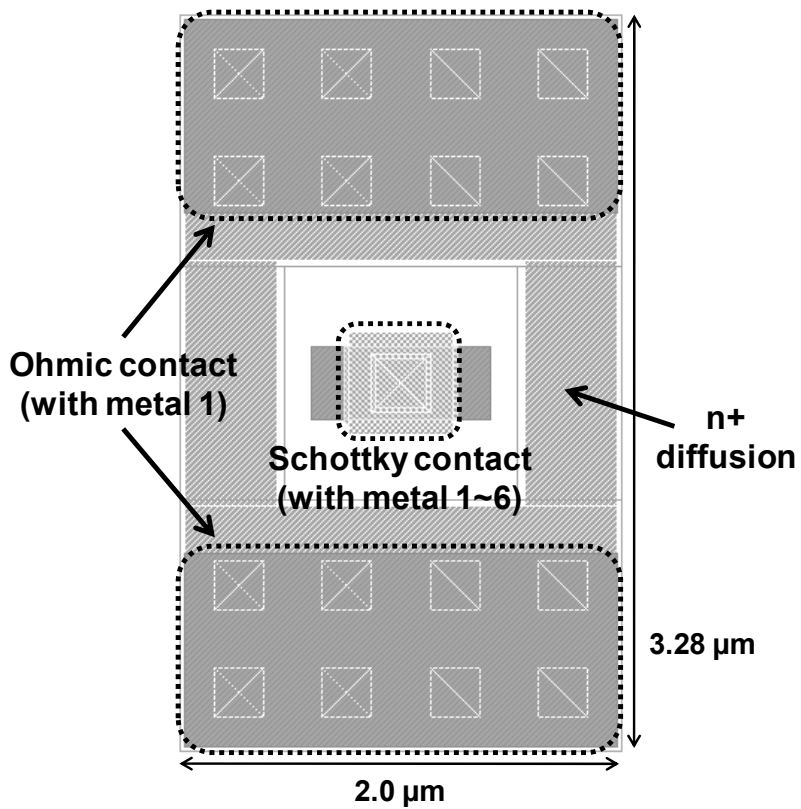
The diode on-resistance is mainly due to the n-well series resistance

because of its low doping. And the diode capacitance comes from the Schottky junction capacitance and the contact parasitic capacitance between the anode metal and the cathode metal. To increase the cut-off frequency, the resistance and the capacitance of the SBD should be minimized. To minimize the junction capacitance, the Schottky contact area was chosen a minimum value of $0.46 \times 0.46 \mu\text{m}^2$ allowed by the $0.18\text{-}\mu\text{m}$ CMOS technology. For the reduction of the parasitic capacitance, spacing between the anode metal and the cathode metal was apart enough by $0.6 \mu\text{m}$. To reduce the resistance at the n-well region, spacing between the Schottky contact region and the ohmic contact region was chosen a minimum value of $0.32 \mu\text{m}$. The total area of the cell was $3.28 \times 2.0 \mu\text{m}^2$.

In practice, this single SBD cell cannot be used alone because the small Schottky contact area limits the current flowing through the SBD, and the series resistance of the cell is too large. Thus, multiple SBD cells connected in parallel were used. The N cells make the resistance and the capacitance to R/N and $C \cdot N$, so the cut-off frequency is kept the same value. In this work, 25 SBD cells in parallel were used as shown in Figure II.5. The total area of the 25-cell SBD is $20.0 \times 14.6 \mu\text{m}^2$. With these considerations, 25-cell SBDs were fabricated in the standard $0.18\text{-}\mu\text{m}$ CMOS technology.



(a)



(b)

Figure II.4 SBD cell: (a) cross-sectional view (b) layout

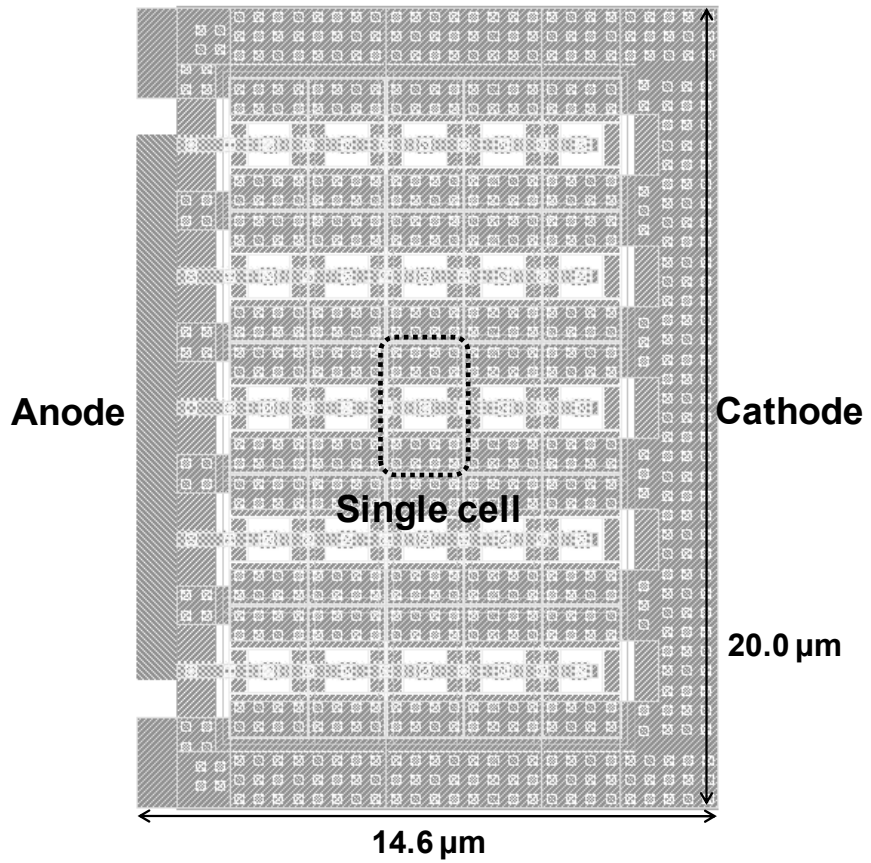


Figure II.5 Layout of 25 SBD cells connected in parallel

II-3. Modeling of Schottky Barrier Diodes

Because SBDs in CMOS technologies are not standard elements, modeling of them should be preceded for circuit design. Figure II.6 shows an equivalent circuit model of the SBD. The nonlinear junction conductance, $g_j(V_j)$, is induced from the ideal diode equation [12],

$$g_j(V_j) = \frac{d}{dV} I_d(V_j) = \frac{q}{\eta KT} I_0 \exp\left(\frac{qV_j}{\eta KT}\right) \quad (2-2)$$

where

I_0 reverse saturation current

V_j junction voltage

η ideality factor

And the nonlinear junction capacitance, $C_j(V_j)$, is represented by

$$C_j(V_j) = \frac{C_{j0}}{\sqrt{1 - V_j / \phi_{bi}}} \quad (2-3)$$

where

C_{j0} zero-biased junction capacitance

ϕ_{bi} built-in voltage

The series resistance, R_s , is mainly due to the n-well resistance, and the parasitic capacitance and inductance, C_{para} and L_{para} , are due to interconnect at the anode and the cathode.

To extract these parameters and to set the equivalent circuit model, DC I-V characterization and RF S-parameter characterization were performed on the 1-port on-wafer measurements as shown Figure II.7. DC measurements were performed by using a semiconductor parameter analyzer, and RF measurements were performed by using a 50-GHz network analyzer.

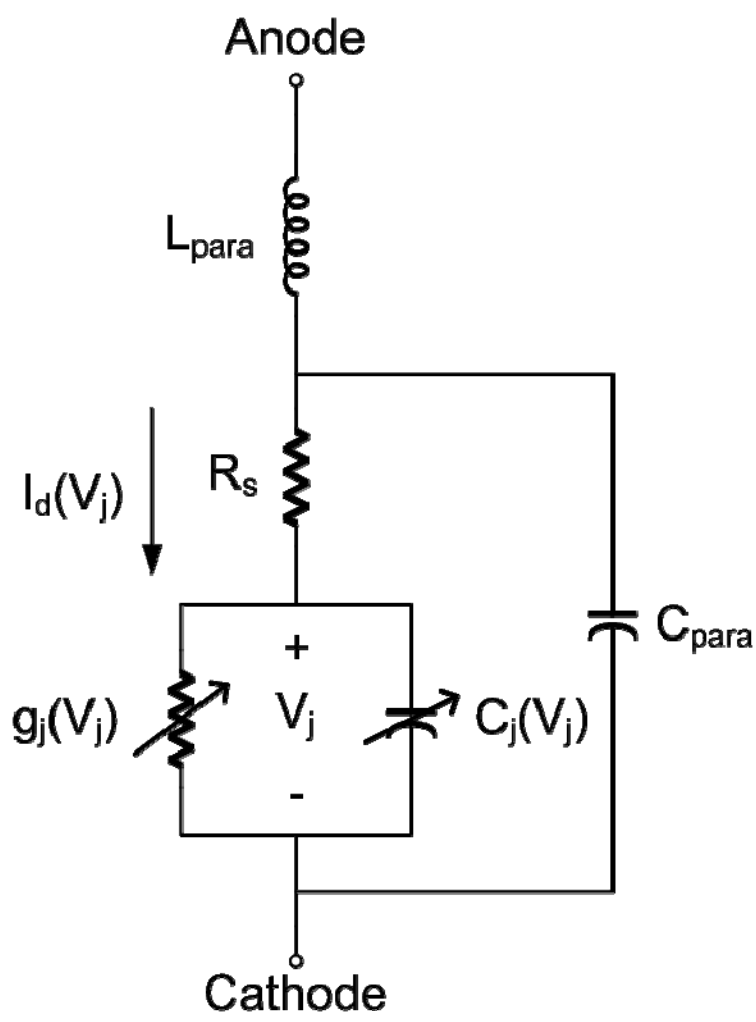


Figure II.6 Equivalent circuit model of SBD

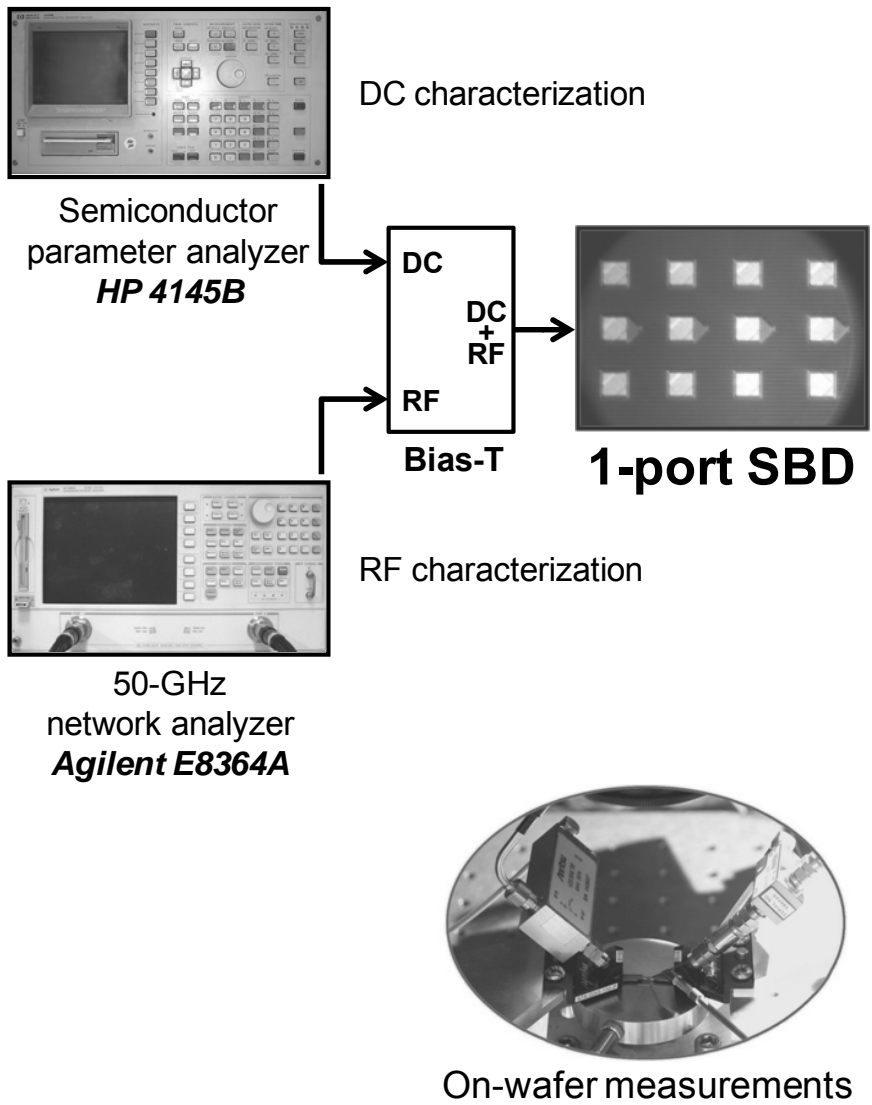


Figure II.7 Measurement setup for characterization of SBD

II-3-A. DC Characterization of Schottky Barrier Diodes

The measured plot in Figure II.8 shows the DC I-V curve of the fabricated 25-cell SBD. It is observed that the fabricated SBD operates well like a general SBD. At the small forward-biased region, the diode current is an exponentially increased function of the diode voltage. And this increase is degraded at the large forward-biased region because of the series resistance of the diode. At the reverse-biased region, the large leakage current is observed due to the Schottky barrier lowering [9]. Therefore, the I-V nonlinearity at the small forward-biased region is applicable for the use for the mixer.

Some diode parameters, which are the ideality factor, the reverse saturation current, and the series resistance, can be obtained by the I-V curve [12]. At the first step, each parameter was calculated from the measured curve by using following equations.

The ideality factor:

$$\eta = \frac{q}{KT} \frac{V_2 - V_1}{\ln I_2 - \ln I_1} \quad (2-4)$$

The reverse saturation current:

$$I_0 = I(V_1) \exp\left(\frac{-qV_1}{\eta KT}\right) \quad (2-5)$$

The series resistance:

$$R_s = \frac{\Delta V_R}{I_R} \quad (2-6)$$

Then, fitting between the measured curve and the simulated curve with calculated parameters was performed. The fitted DC I-V curve of the SBD is shown in Figure II.8. Fitting was performed successfully at the small forward-biased region. At the large forward-biased region of 0.7 V above, however, two curves did not fit. It was observed that the diode resistance increased as the diode voltage increases by unknown factors. And the reverse-biased region was not considered in this model because applications by using the fabricated SBD will be operated in only the forward-biased region. Final fitted parameter values in DC characterization were $\eta = 1.78$, $I_0 = 215 \text{ nA}$, and $R_s = 46.5 \Omega$.

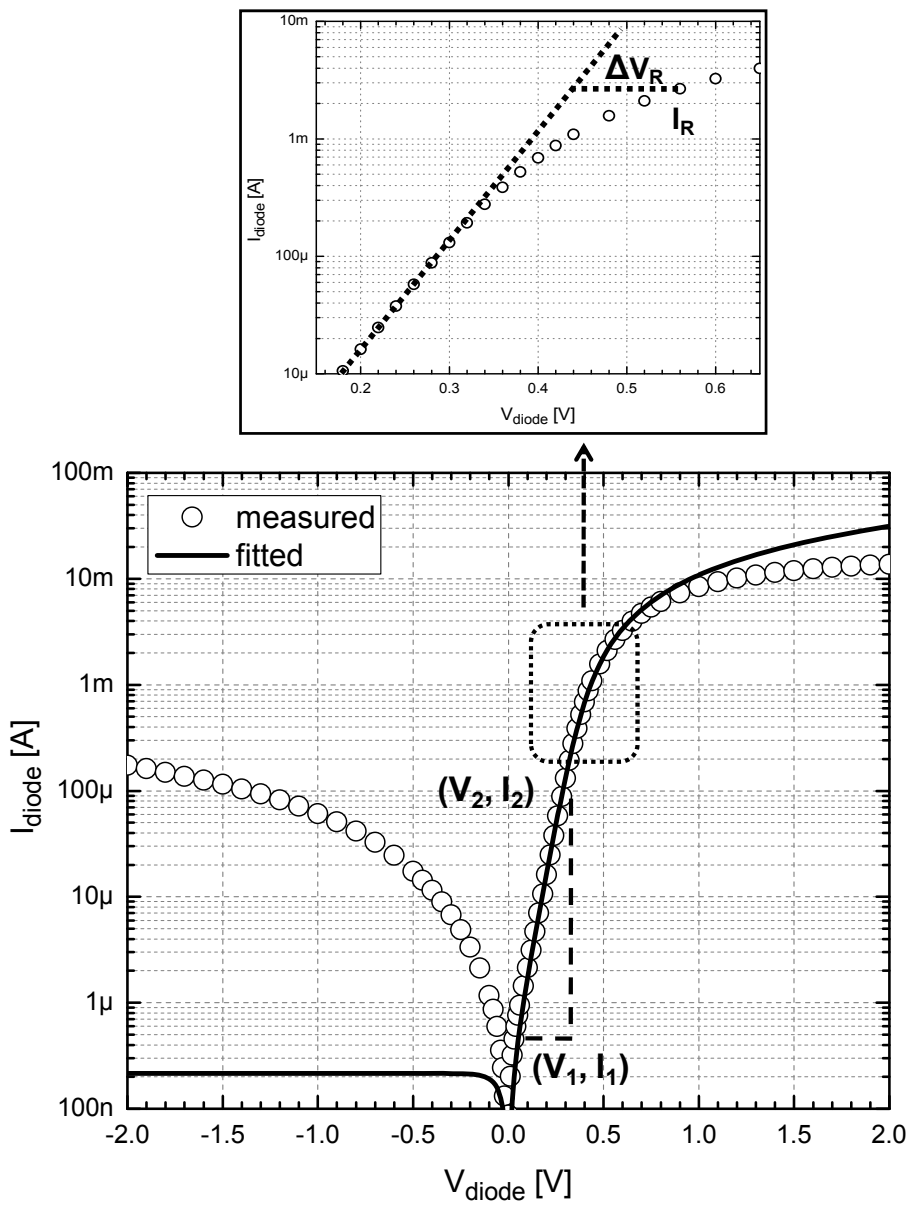


Figure II.8 Measured and fitted DC I-V curves of SBD

II-3-B. RF Characterization of Schottky Barrier Diodes

In RF characterization, extrinsic components of the SBD structure such as a pad and an interconnect line affect the measured results. To minimize them, shield-based pads and ground shield were used [13]. And the pad-open-short deembedding technique was also used for accurate parameter extraction of intrinsic devices in very high frequencies range up to 50 GHz [14].

Figure II.9 shows the diode on-resistance and capacitance of the 25-cell SBD structure in the frequency range of 15 ~ 45 GHz when the diode voltage is zero. They were obtained from measured one-port S-parameter. The measured diode resistance and capacitance were about 20 Ω and 32 fF with slight variations. The diode on-resistance is different from the series resistance of the diode, and is smaller than the series resistance due to the effect of the parasitic capacitance. The measured cut-off frequency was approximately 250 GHz.

To complete the equivalent circuit model of the SBD, extraction of other unknown parameters which are the junction capacitance, the parasitic capacitance, the parasitic inductance, and the built-in voltage was done by fitting S-parameter with frequencies up to 50 GHz. Simulation was performed with the equivalent circuit model as

mentioned in Figure II.6, and parameters obtained in the DC characterization. Figure II.10 shows fitted S-parameter between the measured data and the simulated data. Within the diode voltage of 0 ~ 0.5 V, the simulated results fit well with the measured results.

Final extracted parameters of the SBD in the equivalent circuit model through DC and RF characterizations are listed in Table II.1. The overall performance of the SBD is poor because of the limitation of the fabrication process, the fixed standard CMOS technology.

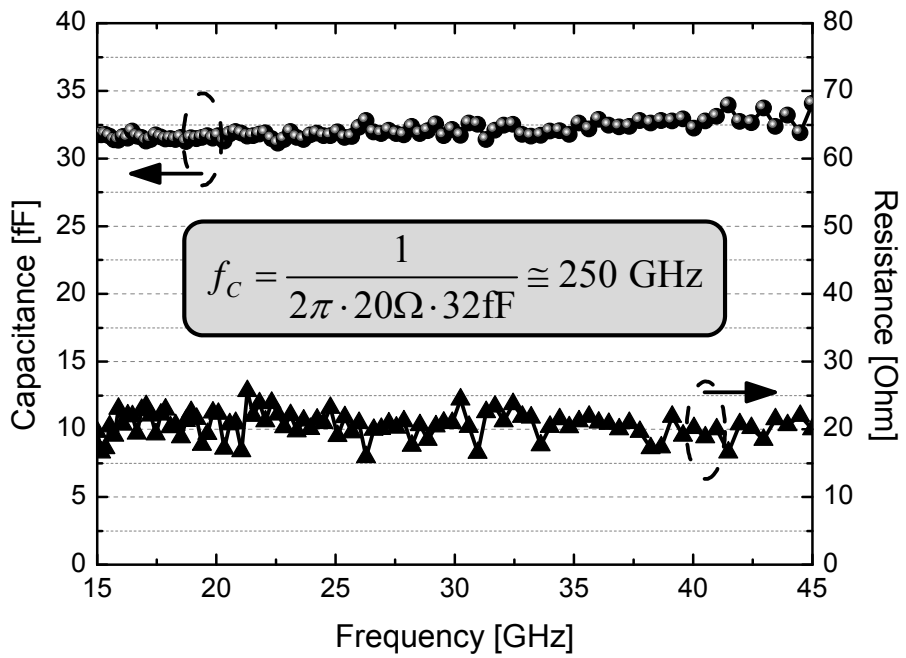


Figure II.9 Measured diode resistance and capacitance of fabricated SBD versus frequency (when diode voltage is zero)

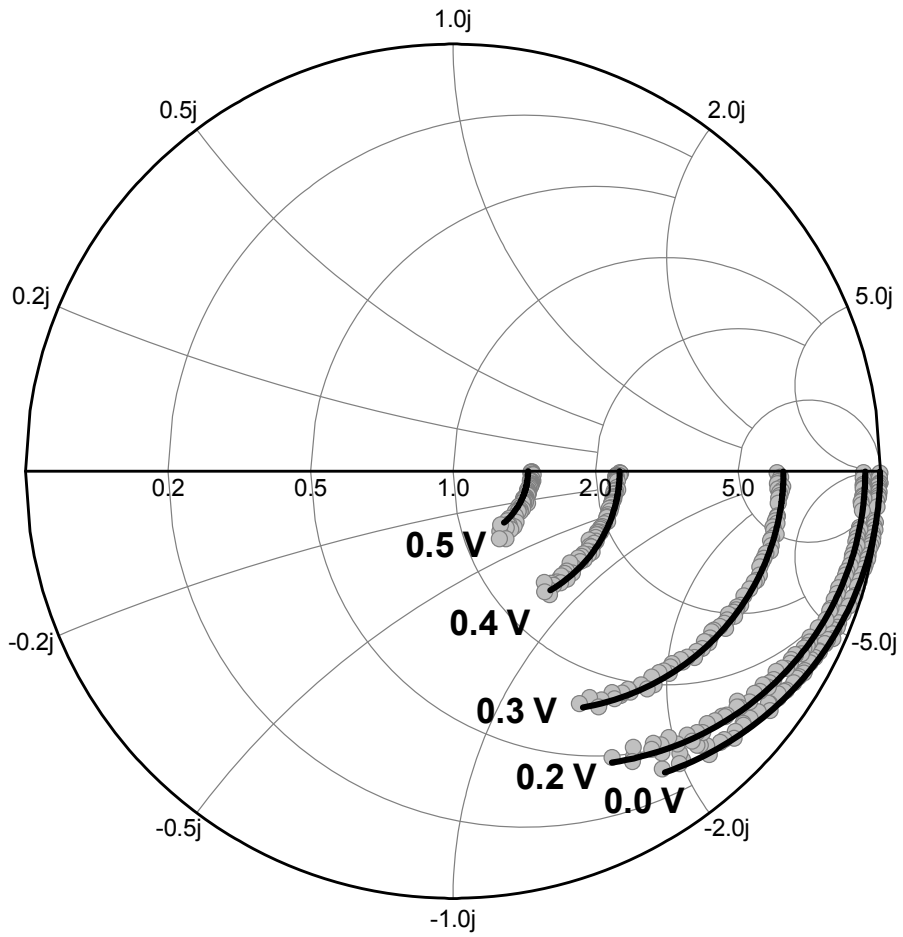


Figure II.10 Measured and fitted S-parameters of SBD (when diode voltage is 0.0, 0.2, 0.3, 0.4, and 0.5 V)

Parameter	Value
Ideality factor	1.78
Reverse saturation current	215 nA
Series resistance	46.5 Ω
Junction capacitance	19.5 fF
Parasitic capacitance	12.5 fF
Parasitic inductance	24 pH
Built-in voltage	0.48 V

Table II.1 Extracted parameters of SBD

III. 60-GHz Square-Law Down-Conversion Mixer

III-1. Design of 60-GHz Mixer Using Schottky Barrier Diodes

A 60-GHz square-law down-conversion mixer using Schottky barrier diodes was designed and fabricated in the 0.18- μm standard CMOS technology. Figure III.1 and Figure III.2 show the schematic and the chip photo of the mixer. The area of the mixer is 1290x450 μm^2 . The mixer is a single diode mixer based on shunt diode configuration using 25-cell SBD. Because the mixer will be applied to 60-GHz self-heterodyne or ASK systems, there is one input port for the RF signal and the LO signal. And, the 1-V bias voltage, V_b , should be applied to the SBD to obtain conversion efficiency without the large LO pump power. The bias circuit is simply configured by using a 2-k Ω N+ poly resistor, R_b .

A 100-fF coupling capacitor, C_c , and a low-pass filter (LPF) are used to isolate each port. The LPF is designed to have a cut-off frequency of 4.5 GHz and high rejection at 60 GHz. 800-fF capacitors and a 3-nH inductor are used for the LPF. All capacitors and inductors are fabricated using metal-insulator-metal (MIM) capacitors and spiral

inductors. Transmission lines, T_1 and T_2 , are microstrip lines for matching networks. Microstrip lines are realized using a top-metal layer for signal lines and a metal-1 layer for a ground plane. T_1 is an input conjugate matching network including $50\text{-}\Omega$ transmission lines and an open stub. And T_2 is a quarter-wavelength line at 60 GHz to transform low input impedance of the LPF to high impedance at 60 GHz [15]. Inductors and transmission lines were accurately designed by using the EM simulator, ADS Momentum. And, an external DC blocker is added at the IF output port to block the DC path to this port through the LPF.

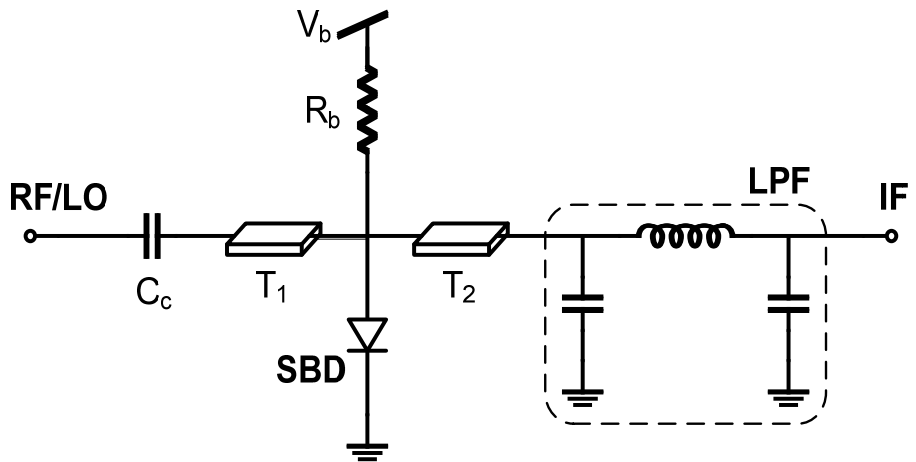


Figure III.1 Schematic of 60-GHz down-conversion mixer

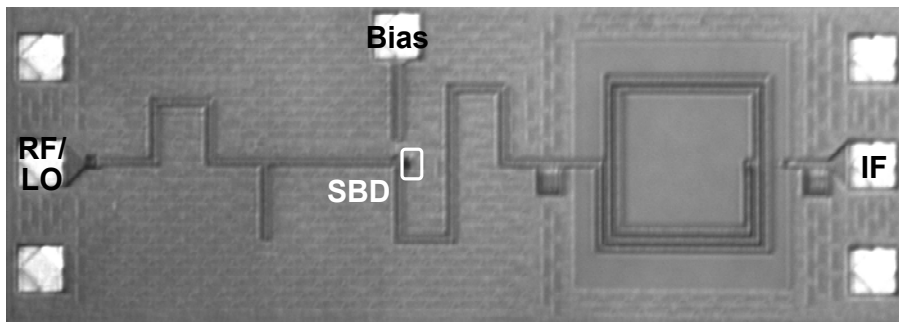


Figure III.2 Chip photo of fabricated 60-GHz down-conversion mixer

III-2. Passive Components for 60-GHz Mixer

Some passives such as the 50- Ω microstrip line and the LPF were fabricated as individual devices to measure their performance separately. Measurements were performed at the frequencies up to 50 GHz by using the 50-GHz network analyzer.

Figure III.3, Figure III.4, and Figure III.5 show simulated and measured results about the characteristic impedance, the electrical length, the insertion loss of the fabricated $\lambda_{60\text{GHz}}/4$, 50- Ω microstrip line having the width of 9.5 μm and the length of 600 μm . The measured characteristic impedance decreases more than the simulated characteristic impedance for higher frequencies. The measured characteristic impedance at 50 GHz is about 47 Ω , and it is expected about 45 Ω at 60 GHz. The measured electrical length is shorter than the simulated result. It is expected about 80 deg at 60 GHz. The insertion loss is below 0.4 dB over frequencies up to 50 GHz.

The LPF was also measured its frequency response as shown Figure III.6. For lower frequencies less than 20 GHz, simulated and measured results are exactly same. Its insertion loss is 0.9 dB, and 3-dB cut-off frequency is 4.7 GHz. For higher frequencies, the measured results are inaccurate, but rejection at 60 GHz is more than 30 dB.

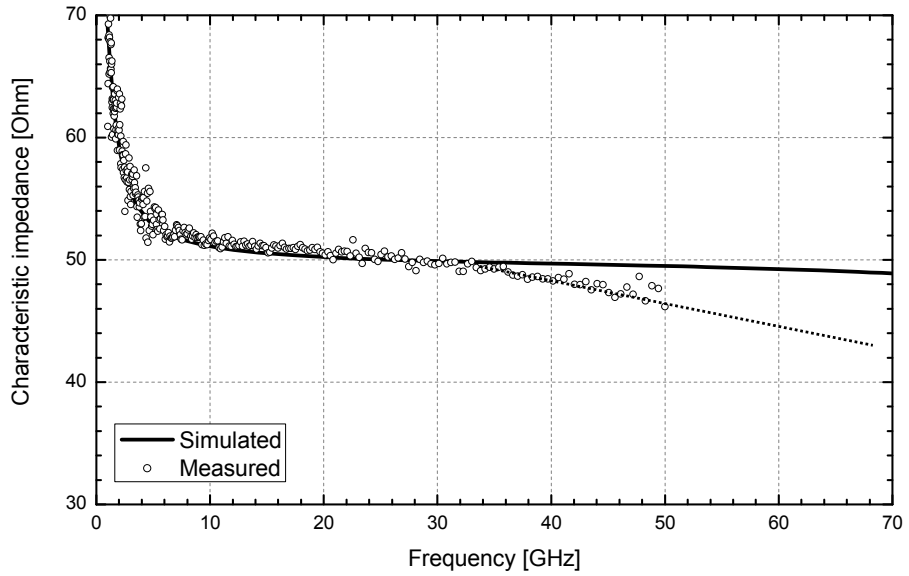


Figure III.3 Characteristic impedance of $\lambda_{60GHz} / 4$, 50- Ω microstrip line

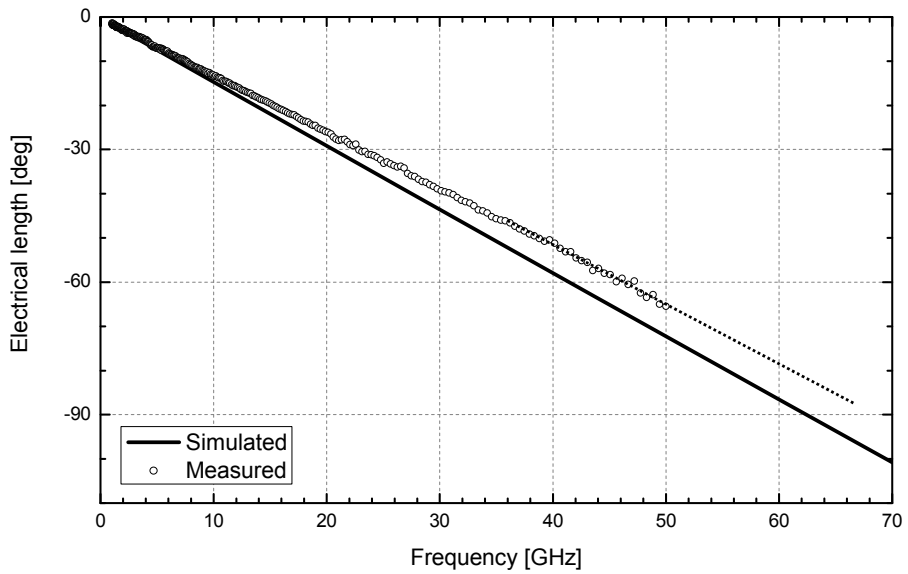


Figure III.4 Electrical length of $\lambda_{60GHz} / 4$, 50- Ω microstrip line

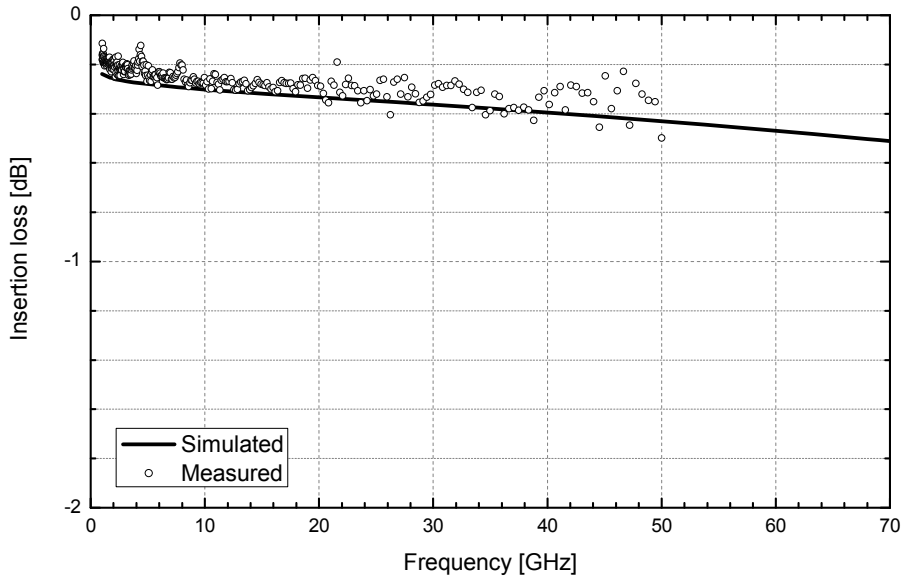


Figure III.5 Insertion loss of $\lambda_{60\text{GHz}}/4$, 50- Ω microstrip line

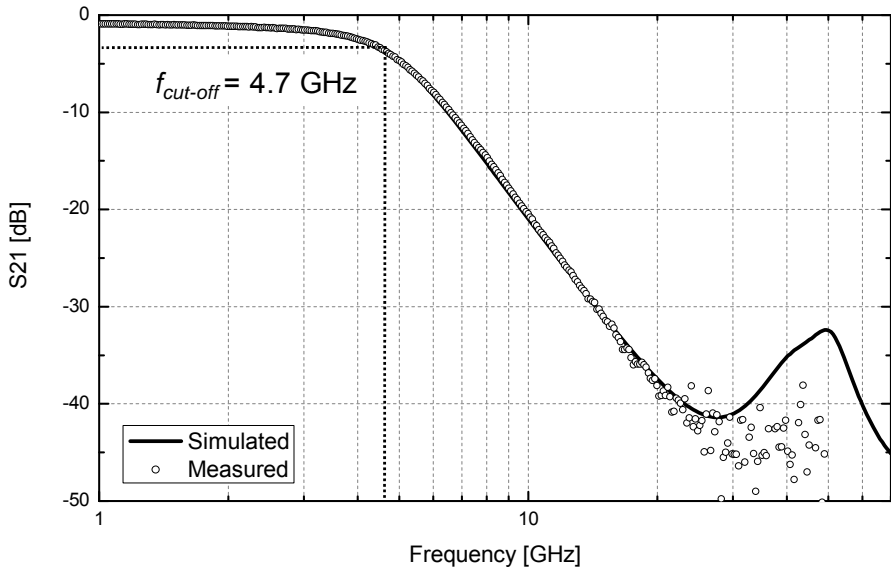


Figure III.6 Frequency response of fabricated LPF

III-3. Performance of 60-GHz Mixer

The fabricated 60-GHz down-conversion mixer using SBDs at the bias voltage of 1 V was measured by on-wafer measurements. At first, its S-parameter was obtained for the input/output return loss characteristic at frequency range up to 50 GHz. Figure III.7 (a) shows input return loss at the RF/LO port. In simulated results, return loss of below -10 dB is achieved in frequencies of 58 ~ 64 GHz. However, measured input return loss couldn't be confirmed in these frequencies due to limitation of experimental equipments. It is merely expected that measured results will be similar to simulated results. Figure III.7 (b) shows output return loss at the IF port. It is not achieved below -10 dB in frequencies less than 3 GHz. It comes from mismatch between the diode impedance and the output port impedance due to the large series resistance, and it can be overcome by integrating baseband circuits at the output port of the mixer.

The conversion loss of the mixer was also measured. A simple view of the experimental setup for this measurement is shown in Figure III.8. The 60-GHz LO and RF signals are generated by a 60-GHz mixer having large LO leakage. The RF input power is tuned to be same power as the LO input power by controlling the IF signal generator

power. And, variable attenuators are used to sweep the input power to the fabricated mixer. DC blocker having DC cut-off frequency of 100 kHz is used at the fabricated mixer output to block DC path to the output port. In this setup, the mixer input signal can have non-flat frequency response and nonlinear distortion products. And, probes and cables connecting the mixer give additional loss. Therefore, the mixer input signal should be accurately examined and deembedded from the measured results.

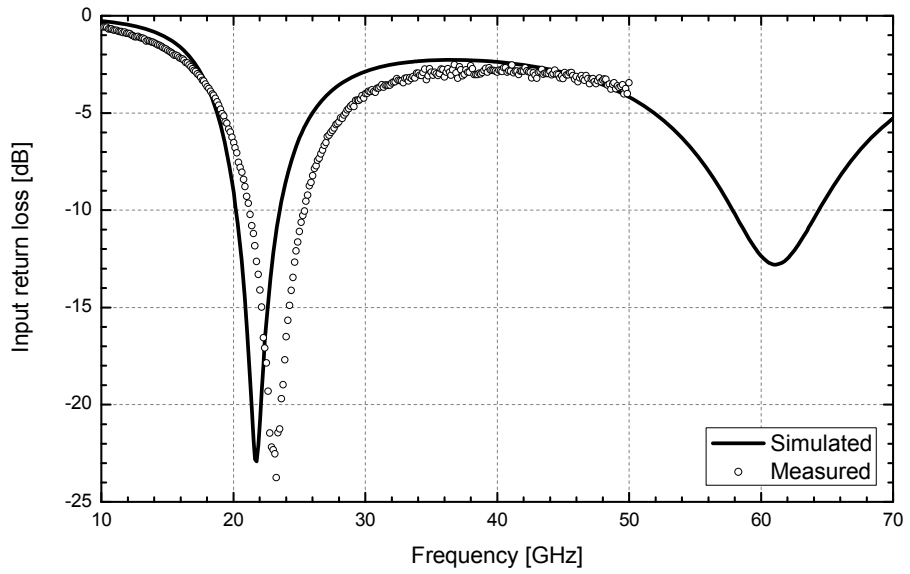
Figure III.9 shows the mixer IF output power and the conversion loss versus the mixer RF input power when the RF frequency is 60.5 GHz. The LO signal is fixed its frequency of 60 GHz, and the LO power is set to same as the RF power. In plots, it is observed that the slope of the IF output power is 2, and the slope of the conversion loss is 1. They are due to the square-law operation, that the LO power increases together with the RF power. The input 1-dB compression point is about -3dBm.

Figure III.10 shows the conversion loss versus the mixer RF input power. The measured peak conversion loss is about -23.7 dB at the input 1-dB compression point of -3 dBm. High conversion loss is due to the high ideality factor and the series resistance of the SBD. In addition, the measured conversion loss is 8 dB less than the simulated result. Performance degradation may be occurred due to uncertainty of

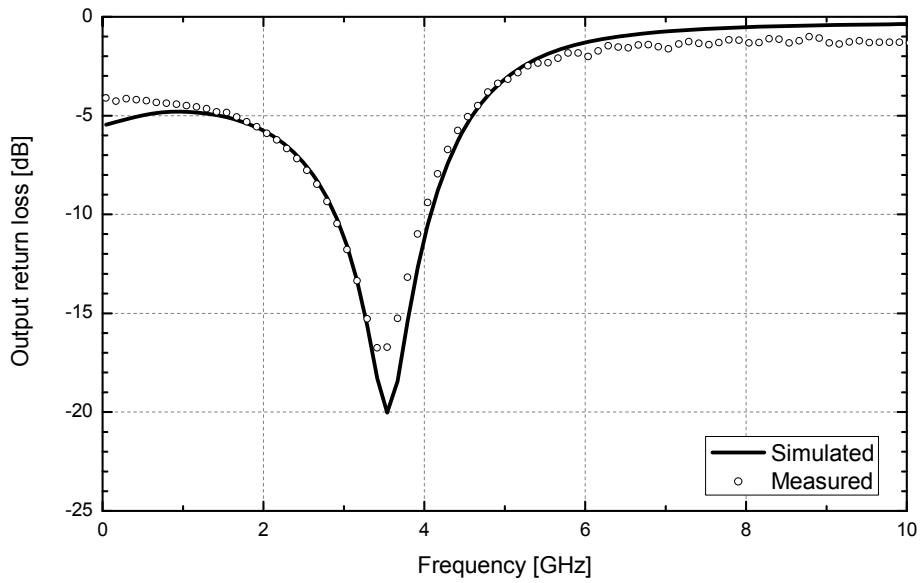
the SBD model.

Figure III.11 shows the conversion loss versus RF frequency when the RF mixer input power is -25 dBm, the linearly operating point. In the frequency range of 60.5 ~ 63.0 GHz, the variation of the conversion loss is within 3 dB. With the DC blocker of cut-off frequency of 100 kHz, it is expected that the operating frequency range of the mixer can cover 100 kHz ~ 3 GHz.

Table III.1 shows the performance summary of the fabricated mixer and comparisons with previous works. The comparisons show that this work has low conversion efficiency, but has large bandwidth at interesting frequency of 60 GHz. The conversion loss will be improved by further study from this initial trial.



(a)



(b)

Figure III.7 Return loss of the mixer: (a) input and (b) output (when bias voltage is 1 V)

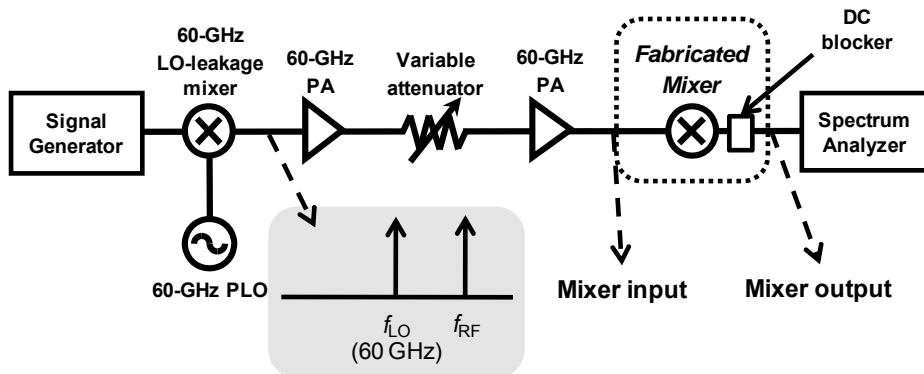


Figure III.8 Experimental setup for measurement of conversion loss of mixer

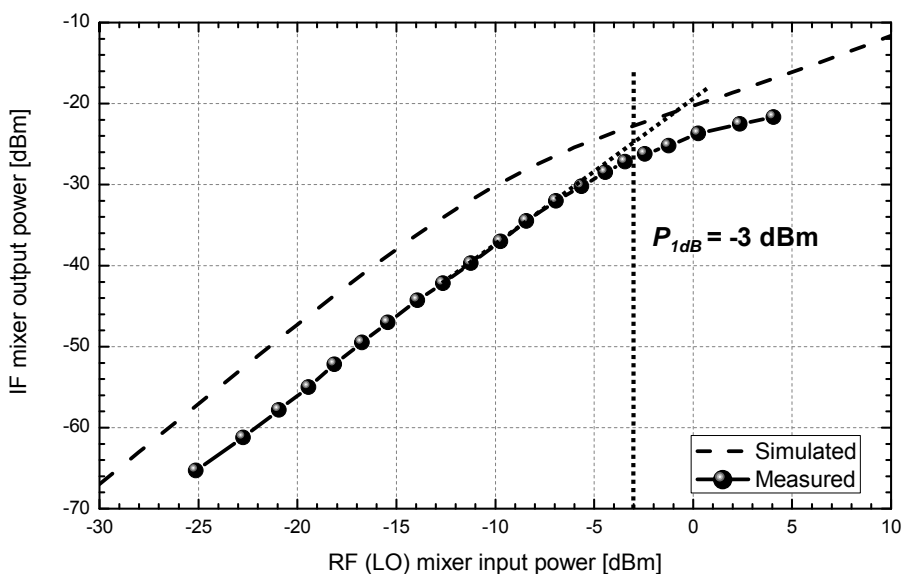


Figure III.9 IF mixer output power versus RF mixer input power (when LO power = RF power and RF frequency of 60.5 GHz)

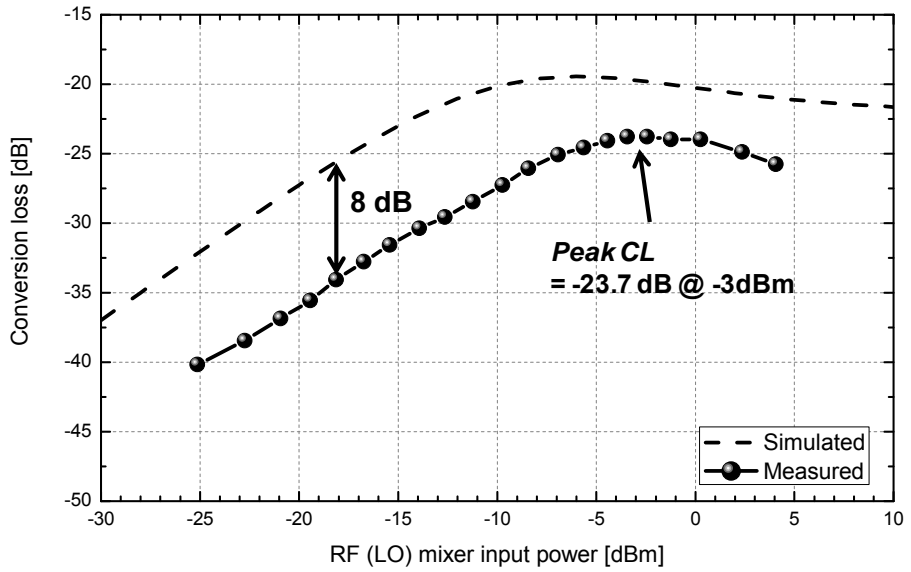


Figure III.10 Conversion loss versus RF mixer input power (when LO power = RF power and RF frequency of 60.5 GHz)

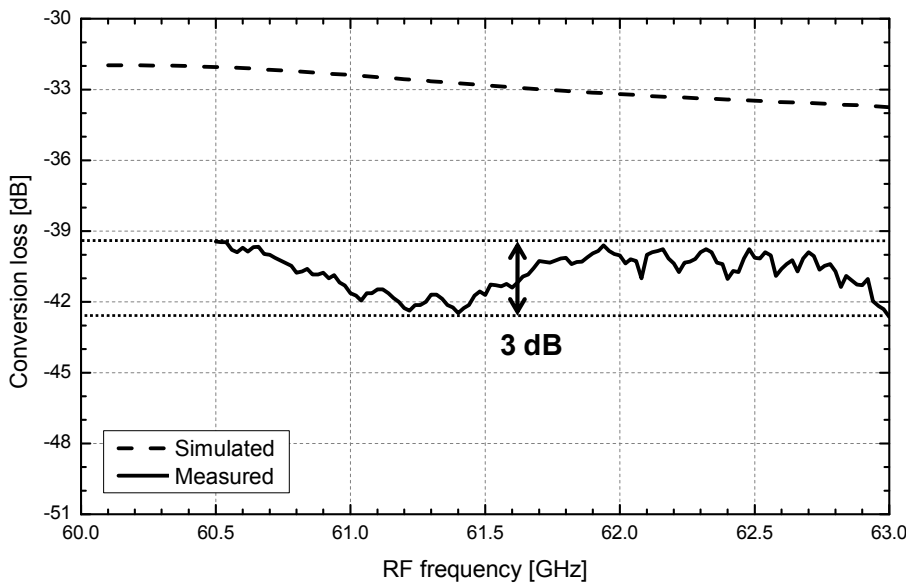


Figure III.11 Conversion loss versus RF frequency (when RF (LO) mixer input power is -25 dBm)

Specification	[16]	[17]	This work
Process technology	0.13- μm CMOS	0.13- μm SiGe BiCMOS	0.18- μm CMOS
Power consumption	8.5 mW	Passive	326 μW
RF frequency	~ 10.3 GHz	120 GHz	58 \sim 64 GHz
IF frequency	~ 1.7 GHz	500 MHz	~ 3 GHz
Peak conversion loss	-2.2 dB (with 8-dB gain LNA)	- 3 dB (LO power of 16 dBm)	-23.7 dB (LO power of -3 dBm)
Input 1-dB compression point	Not reported	Not reported	-3 dBm
Note	LNA+Single diode mixer	APDP mixer	Single diode mixer

Table III.1 Performance summary of fabricated 60-GHz square-law down-conversion mixer and comparisons with pervious works

IV. 60-GHz Communication Demonstrations

Using Fabricated Mixer

IV-1. Principles of Self-heterodyne Systems

In self-heterodyne systems, a power ratio of the received LO and RF signals is an important factor for efficient transmission. The down-converted signal at the receiver is represented by

$$\begin{aligned} v_{IF}(t) &= (\sqrt{2P_{RF}} \cos w_{RF}t + \sqrt{2P_{LO}} \cos w_{LO}t + n(t))^2 \\ &= 2\sqrt{P_{RF}P_{LO}} \cos w_{IF}t \\ &\quad + 2P_{RF} \cos^2 w_{RF}t \\ &\quad + 2\sqrt{2P_{RF}} n(t) \cos w_{RF}t + 2\sqrt{2P_{LO}} n(t) \cos w_{LO}t + n^2(t) \\ &\quad + \dots \end{aligned} \tag{4-1}$$

The first term is the desired down-converted signal. However, the second term, the second-order intermodulation distortion (IM2), is also occurred in the frequency band of DC to double-sideband bandwidth of RF signal, B. For non-overlap between the IF signal and the IM2, the IF frequency should follow this condition [6],

$$f_{IF} \geq \frac{3}{2}B \quad (4-2)$$

On the other hand, the third term in (4-1) acts noise, so degrades a SNR of the down-converted IF signal. In the presence of noise, the SNR of the IF signal can be obtained by [6]

$$SNR = \frac{\frac{R}{(1+R)^2} P_{rcv}^2}{BB_0(kTF)^2 + 2BP_{rcv}kTF} \quad (4-3)$$

where

R LO power to RF power ratio

P_{rcv} total received power

B_0 noise bandwidth

F noise figure of receiver

Therefore, when the total received power is limited, LO power to RF power ratio of 1 is the optimum condition to maximize the SNR of the down-converted IF signal.

$$R = \frac{P_{LO}}{P_{RF}} = 1 = 0 \text{ dB} \quad (4-4)$$

IV-2. Broadband Data Transmission in 60-GHz Self-Heterodyne System

To investigate the feasibility of the fabricated 60-GHz square-law down-conversion mixer for 60-GHz systems, Broadband data transmission in the 60-GHz self-heterodyne system was demonstrated with 622-Mb/s BPSK data. Figure IV.1 shows the experimental setup for 60-GHz self-heterodyne system. The BPSK modulator is realized with a signal generator, a mixer, and filters. The input data is 622-Mb/s NRZ 2^7-1 word length pseudorandom binary sequence (PRBS) provided by a pattern generator. An LPF limits the bandwidth of input data. After that, it is modulated to the BPSK signal using a simple frequency up-conversion technique with the IF frequency of 1.4 GHz. A step attenuator is set up between the BPSK modulator and the RF transmitter in order to control the IF input power.

The 60-GHz RF transmitter is composed of the discrete components which are a 60-GHz mixer, a 60-GHz PLO, a BPF, and a PA. The IF BPSK signal is up-converted to the 60-GHz band with the center frequency of 61.4 GHz. The output of the 60-GHz mixer contains not only RF signal, but also LO signal. And RF signal power is tuned to have same power as LO signal power by controlling the IF step

attenuator. The BPF filters out the lower sideband of the RF signal. Total transmitter output at the PA output is set to 8 dBm. Figure IV.2 shows the transmitter output spectrum containing LO and upper side band RF signals. In this spectrum, intermodulation distortions are occurred beside the RF signal. They are due to nonlinearity of the IF mixer, and can be eliminated the IF BPF.

Variable attenuators between the transmitter and the receiver are substitute for propagation loss between high-gain antennas unconsidered multi-path fading. The RF receiver is simply configured only with a LNA, the fabricated mixer, and an IF amplifier without a local oscillator. After signal amplification by the LNA, the received LO and RF signals are down-converted to the IF band, and then amplified by the IF amplifier. Figure IV.3 shows the received IF output spectra. In Figure IV.3 (a), there exist much IM2 components without the IF BPF. Therefore, they should be filtered out by using the BPF as shown if Figure IV.3 (b).

At the IF output, the down-converted BPSK signal is demodulated to baseband data by the BPSK demodulator having maximum data rate of 622 Mb/s [18]. And a limiting amplifier is added to compensate the sensitivity limit of the BPSK demodulator. The demodulated signal is observed by using a spectrum analyzer and an error detector.

To evaluate the performance of the 60-GHz self-heterodyne link, the

back-to-back link which the IF input is directly connected to the IF output is also demonstrated. The bit error rate (BER) performance is measured changing the propagation loss controlling the 60-GHz variable attenuators.

Figure IV.4 shows BER as a function of the IF output power for 622-Mb/s BPSK data. In the 60-GHz self-heterodyne link, when the IF output power is larger than -23 dBm, error-free transmission (below 10^{-10} BER) is achieved. And the overall BER performance has a power penalty of 8 dB against the back-to-back link. This may come from noise down-converted with the IF signal at the down-conversion mixer.

When error-free transmission is achieved in the 60-GHz link, the propagation loss is about 24 dB. If high directional antennas having antenna gain of 24 dBi available in 60 GHz are used in the link, 1.5-m wireless transmission of 622-Mb/s BPSK data is possible. Though these results, possibility of 60-GHz WPAN systems using mixers based on CMOS SBDs is examined.

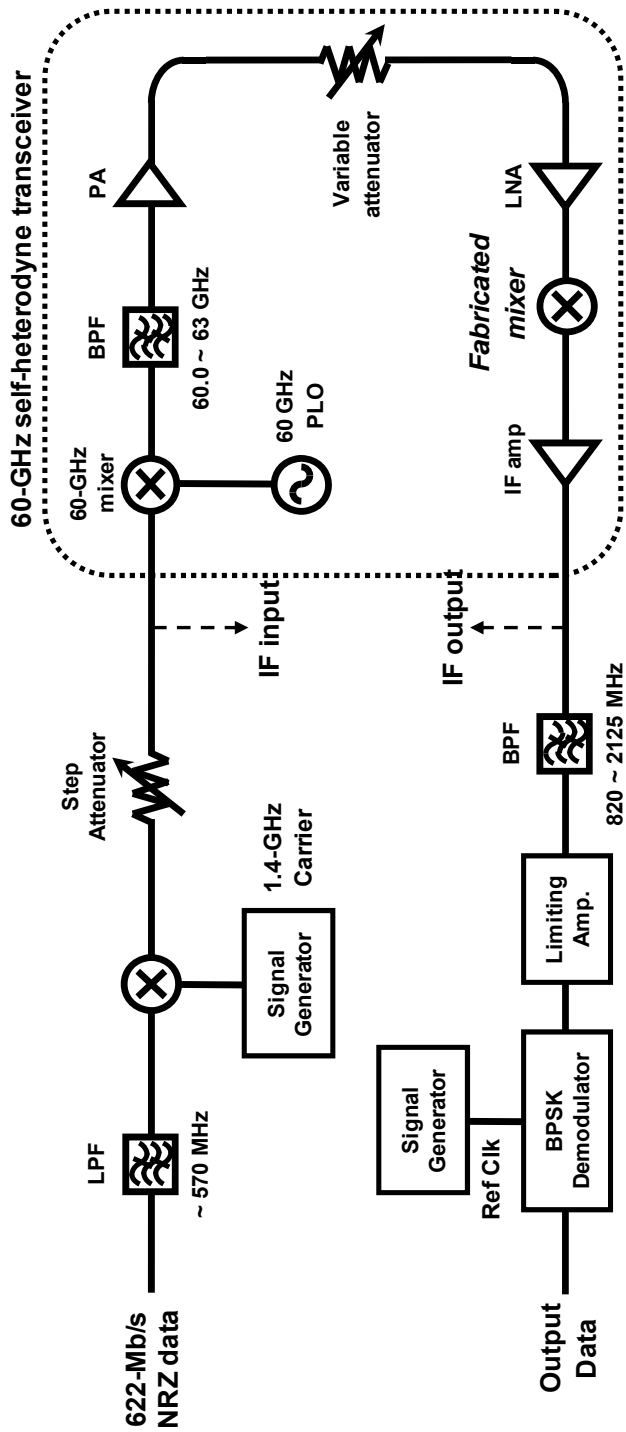


Figure IV.1 Experimental setup for 60-GHz self-heterodyne system

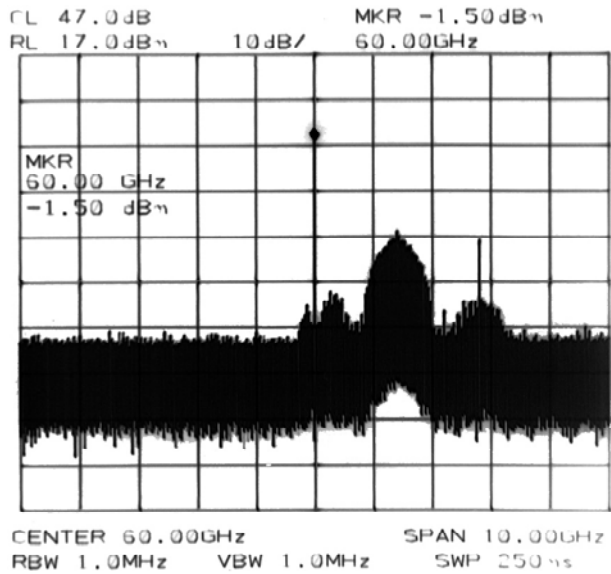


Figure IV.2 60-GHz transmitter output spectrum in self-heterodyne system with LO signal and BPSK-modulated RF signal

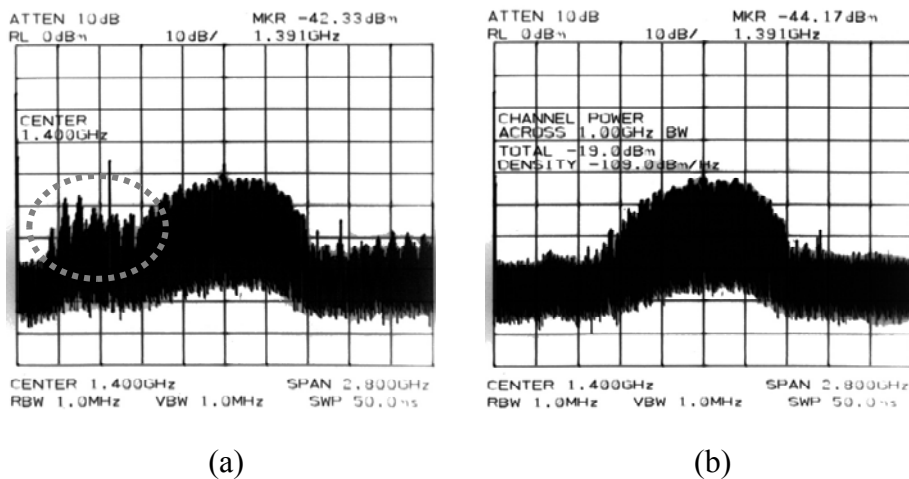


Figure IV.3 Received IF output spectra in self-heterodyne system: (a) without receiver IF BPF and (b) with receiver IF BPF

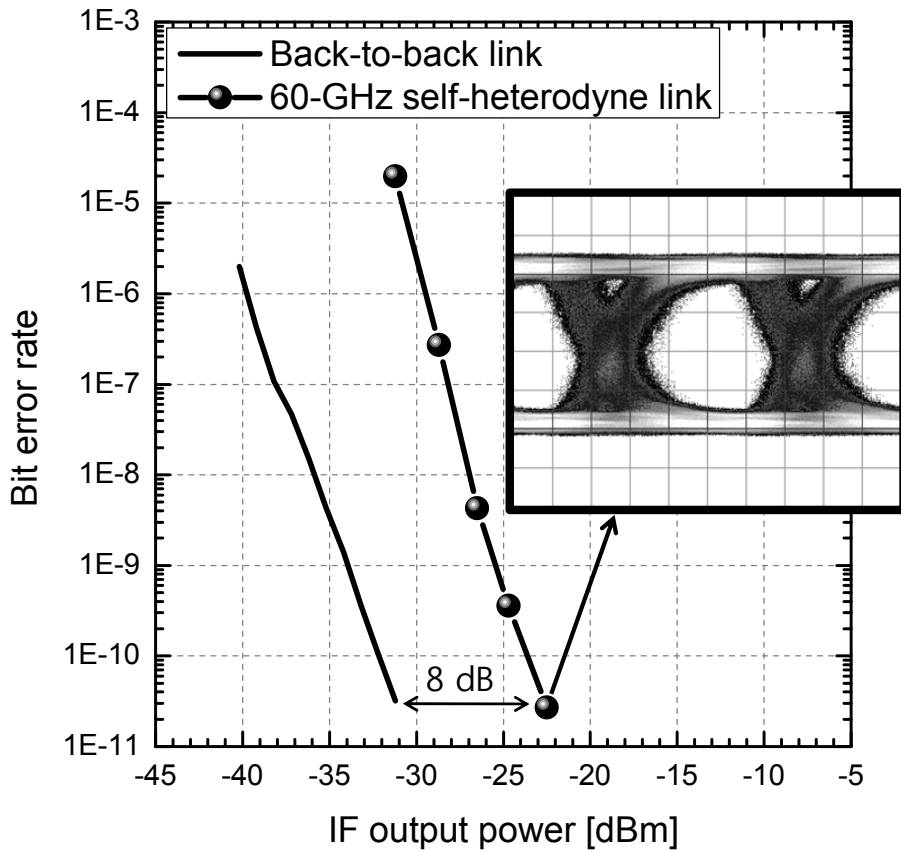


Figure IV.4 Relationship between IF output power and bit error rate for back-to-back link and 60-GHz self-heterodyne link

IV-3. Broadband Data Transmission in 60-GHz ASK System

In the same way with the self-heterodyne system, broadband data transmission in the 60-GHz ASK system was demonstrated with 622-Mb/s baseband data. Figure IV.5 shows the experimental setup for the 60-GHz ASK system. 622-Mb/s input data are directly modulated to the 60-GHz ASK signal using a simple frequency up-conversion technique with a subharmonic mixer. The modulated ASK signal consists of both up-converted baseband signal and the 60.0-GHz LO leakage signal. The powers of these two signals are tuned to have same level by controlling the step attenuator. The total transmitter output signal power at the power amplifier output is set to 9.4 dBm. Instead of antennas, 60-GHz variable attenuators between the transmitter and the receiver are used for accounting for path loss between antennas. The RF receiver is simply configured with a LNA, the fabricated mixer, and a baseband amplifier, without a local oscillator. The performance of transmission is examined using a spectrum analyzer and an error detector. Figure IV.6 shows the spectra of (a) the transmitter output signal and (b) the received baseband signal when the received signal power at the input of 60-GHz receiver is -13 dBm.

Figure IV.7 shows the bit error rate (BER) performance as functions of the total RF received signal power and the corresponding estimated propagation distance. The total RF received signal power was swept by changing the attenuation level of 60-GHz attenuators. The propagation distance is calculated from the attenuation level with the assumption of 24-dBi Tx and Rx directional antennas. The BER performance achieves below 10^{-10} at the RF received signal power higher than -13 dBm, with the propagation loss of 1.3 meters. The inset in Figure IV.7 shows the eye diagram of the received baseband signal at the received signal power of -13 dBm. At the BER of 10^{-6} , which is an acceptable value in the wireless transmission, the calculated propagation distance is about 2.5 meter. For considering one of the mandatory 60-GHz WPAN usage models, file-transfer applications between portable devices require only the distance coverage of 1 meter [19]. Experimental results show that 60-GHz ASK systems using CMOS SBD mixers satisfy the usage model at the data rate of 622 Mb/s.

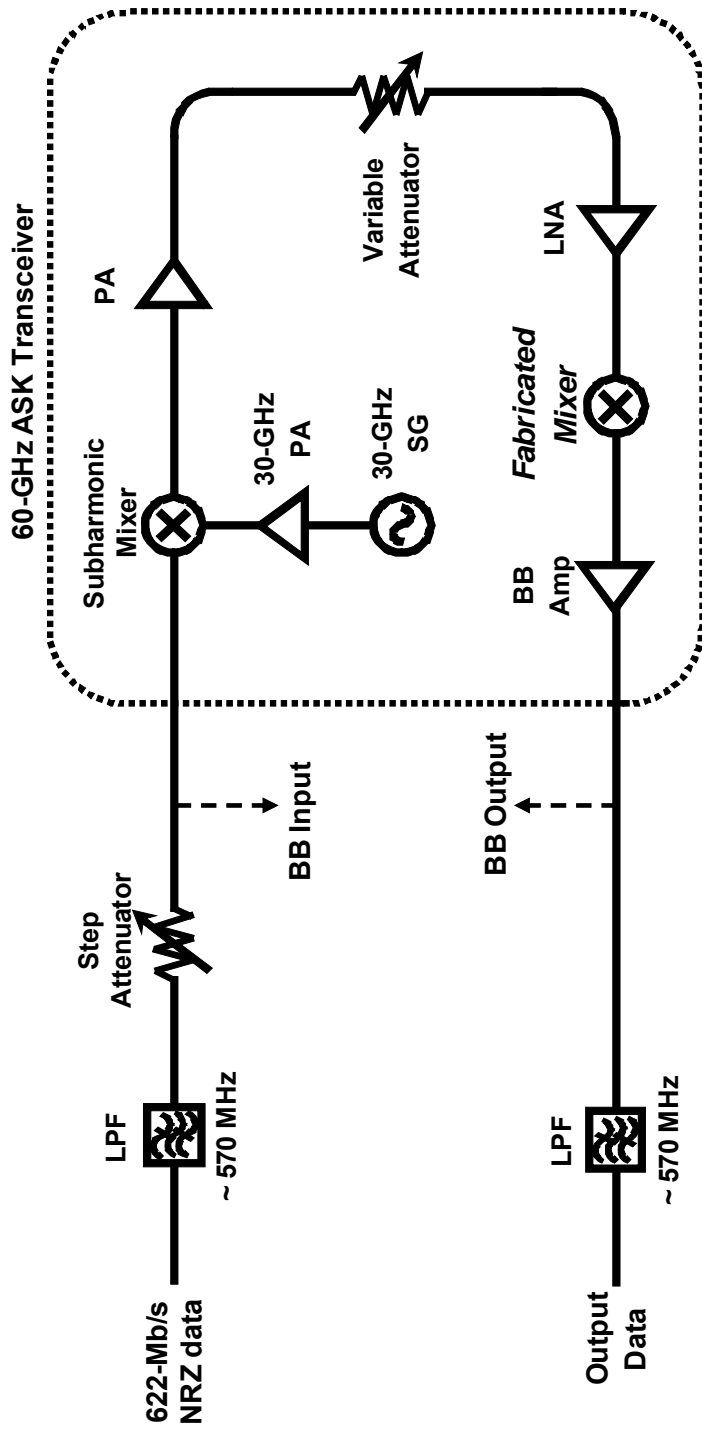
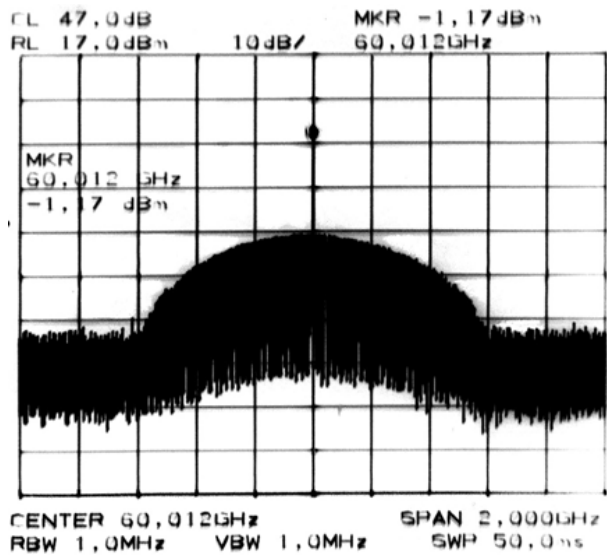
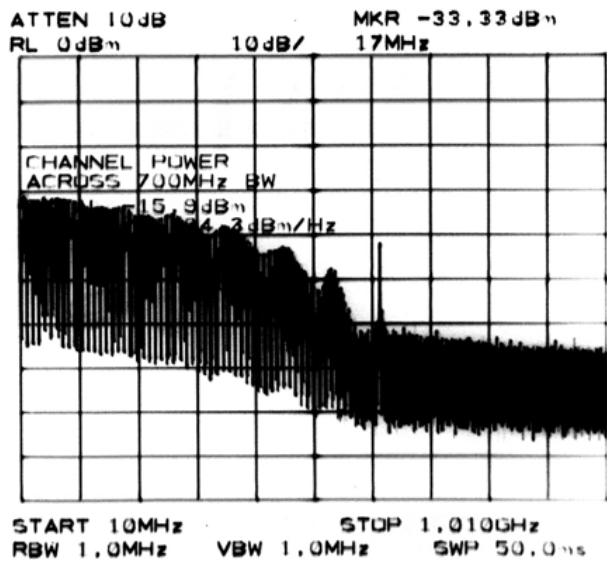


Figure IV.5 Experimental setup for 60-GHz ASK system



(a)



(b)

Figure IV.6 Spectra in 60-GHz ASK system: (a) transmitter output signal and (b) baseband output signal

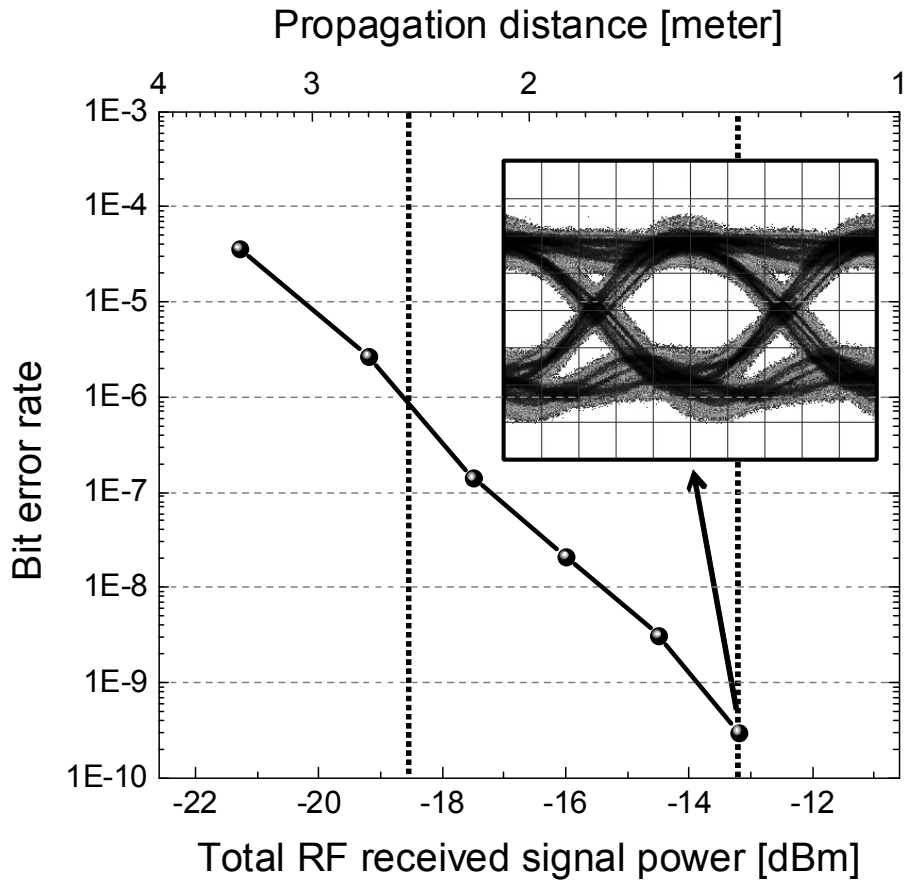


Figure IV.7 BER versus total received signal power and calculated propagation distance for 60-GHz self-heterodyne system (Tx and Rx antenna gain of 24 dBi each)

V. Summary

60-GHz wireless communication, especially IEEE 802.15.3c 60-GHz wireless personal area network has been actively developed for the demand of high data rate transmission. Consequently, low-complexity and low-cost 60-GHz RF transceivers for conventional heterodyne or direct-conversion systems have also investigated in standard CMOS technologies. However, there are some difficulties to develop 60-GHz transceivers on time to market. For that, low-cost and low-complexity self-heterodyne systems and ASK systems can be a very attractive solution due to their simple transceiver configuration with square-law down-conversion at the receiver and robustness of local oscillator phase error and frequency offset.

In this dissertation, the 60-GHz self-heterodyne system was realized by developing a 60-GHz square-law down-conversion mixer. For the mixer, simple diode mixer based on Schottky barrier diodes (SBDs) having the cut-off frequency of hundreds-GHz in CMOS technologies was proposed.

In chapter II, SBDs were fabricated in the standard 0.18- μm CMOS technology, and measured their DC and RF characteristics. And then, the equivalent circuit model of SBDs was proposed for circuit design.

Fabricated SBDs had the cut-off frequency of 250 GHz, and were verified their feasibility of use for 60-GHz down-conversion mixers.

Next, design and results of the 60-GHz square-law down-conversion mixer with simple shunt single diode configuration using fabricated SBDs were explained in chapter III. The fabricated mixer had one input port for LO and RF up-converted signal, and one output port for IF down-converted signal. After design method was described, characteristics of passive components for the mixer, such as the $\lambda_{60\text{GHz}} / 4$, 50- Ω microstrip line and the LPF were examined. And then, input / output matching characteristics and conversion efficiency characteristics of the fabricated were examined. Its peak conversion loss was -23.7 dB when the LO and RF frequencies were 60 GHz and 60.5 GHz and each LO power and RF power was -3 dBm. Conversion loss over the frequency band of 60.5 ~ 63.0 GHz was flat with variation of less than 3 dB. Output 1-dB compression point was -3 dBm. In results, some questions were occurred. One was bad IF output return loss of -5 dB due to impedance mismatch between the diode and the IF output port. The other was that the measured conversion loss was 8 dB lower than the simulated conversion loss. This may come from uncertainty of the SBD model, the impedance mismatch, and the implementation loss. They should be solved through further studies.

Finally, demonstration of 60-GHz communication using the fabricated mixer was performed in chapter IV. At first, principles of self-heterodyne systems were analyzed in terms of effect of IM2 and LO and RF power ratio for maximum SNR. And then, 622-Mb/s BPSK data transmission in the 60-GHz self-heterodyne system was demonstrated. Error-free transmission was achieved at the propagation loss of 24 dB, 1.5-meter calculated propagation distance with 24-dBi high-gain antennas. 622-Mb/s data transmission in the 60-GHz ASK system was also demonstrated. Error-free transmission was achieved at the propagation loss of 22 dB, 1.3-meter distance.

Square-law down-conversion mixers based on SBDs in standard CMOS technologies are very helpful for simplifying receivers in self-heterodyne systems and ASK systems. With further improvement in design techniques, mixers based on SBDs will be an interesting solution to be faster time to market of 60-GHz WPAN communications.

References

- [1] *IEEE 802.15 WPAN Millimeter Wave Alternative PHY Task Group 3c*, <http://www.ieee802.org/15/pub/TG3c.html>
- [2] *Performance Characteristics of 60-GHz Communication Systems*, Terabeam Corporation, 2002
- [3] David Alldred, Brian Cousins, and Sorin P. Voinigescu, *A 1.2V, 60-GHz Radio Receiver with On-Chip Transformers and Inductors in 90-nm CMOS*, IEEE Compound Semiconductor Integrated Circuit Symposium, pp. 51-54, Nov. 2006
- [4] Behzad Razavi, *CMOS Transceivers at 60 GHz and Beyond*, IEEE International Symposium on Circuits and Systems, pp. 1983-1986, May 2007

- [5] Chang-Soon Choi, Yozo Shoji, Hiroshi Harada, Ryuhei Funada, Shuzo Kato, Kenichi Maruhashi, Ichihiko Toyoda, and Kazuaki Takahashi, *RF Impairment Models for 60-GHz-band SYS/PHY Simulation*, IEEE P802.15 Working Group for Wireless Personal Area Networks (WPANs), doc. IEEE 802.15-06-0477-01-003c, Nov. 2006
- [6] Yozo Shoji, Kiyoshi Hamaguchi, and Hiroyo Ogawa, *Millimeter-Wave Remote Self-Heterodyne System for Extremely Stable and Low-Cost Broad-band Signal Transmission*, IEEE Transactions on Microwave Theory and Techniques, Vol. 50, No. 6, pp. 1458-1468, June 2002
- [7] Bruce Bosco, Paul Gorday, Steve Rockwell, Adam Rentschler, and Robert Pauley, *Low Cost, Low Complexity ASK-Based PHY for 802.15.3c*, IEEE P802.15 Working Group for Wireless Personal Area Networks (WPANs), doc. IEEE 802.15-07-0695-02-003c, May 2007
- [8] S. Sankaran and K. K. O, *Schottky Diode with Cutoff Frequency of 400 GHz Fabricated in 0.18 μ m CMOS*, Electronics Letters, Vol. 41, No. 8, pp. 506-508, Apr. 2005

- [9] Robert F. Pierret, *Semiconductor Device Fundamentals*, Addison-Wesley Publishing Company, 1996
- [10] E. Bucher, S. Schulz, M. Ch. Lux-Steiner, P. Munz, U. Gubler, and F. Greuter, *Work Function and Barrier Heights of Transition Metal Silicides*, Applied Physics A, Vol. 40, pp. 71-77, 1986
- [11] R.M. Rassel, J.B. Johnson, B.A. Orner, S.K. Reynolds, M.E. Dahlström, J.S. Rascoe, A. J. Joseph, B.P. Gaucher, J.S. Dunn, and S.A. St. Onge, *Schottky Barrier Diodes for Millimeter Wave SiGe BiCMOS Applications*, Bipolar/BiCMOS Circuits and Technology Meeting, 2006
- [12] Stephen A. Maas, *Microwave Mixers*, 2nd ed., Artech House, 1993
- [13] Troels Emil Kilding, *Shield-Based Microwave On-Wafer Device Measurements*, IEEE Transactions on Microwave Theory and Techniques, Vol. 49, No. 6, pp. 1039-1044, June 2001

- [14] Luuk F. Tiemeijer, Ramon J. Havens, Andre B. M. Jansman, and Yann Bouttement, *Comparison of the “Pad-Open-Short” and “Open-Short-Load” Deembedding Techniques for Accurate On-Wafer RF Characterization of High-Quality Passives*, IEEE Transactions on Microwave Theory and Techniques, Vol. 53, No. 2, pp. 723-729, Feb. 2005
- [15] Eric Chan, *Design of a 5-6 GHz Single Balanced Schottky Diode Mixer*, Asia-Pacific Conference on Applied Electromagnetics, pp. 67-71, Aug. 2003
- [16] S. Sankaran and K. K. O, *A Ultra-Wideband Amplitude Modulation (AM) Detector Using Schottky Barrier Diodes Fabricated in Foundry CMOS Technology*, IEEE Journal of Solid-State Circuits, Vol. 42, No. 5, pp. 1058-1064, May 2007
- [17] C. Mishra, U. Pfeiffer, R. Rassel, and S. Reynolds, *Silicon Schottky Diode Power Converters Beyond 100 GHz*, IEEE Radio Frequency Integrated Circuits Symposium, pp. 547-550, June 2007

- [18] Duho Kim, Woo-young Choi, Young-kwang Seo, Hyunchin Kim, *A Novel BPSK Demodulating Scheme Using a Half-rate Bang-bang Phase Detector*, International SoC Design Conference, No. 5.2, pp. 87-90, Oct. 2006
- [19] A. Sadri, *802.15.3c Usage Model Document (UMD), Draft*, IEEE P802.15 Working Group for Wireless Personal Area Networks (WPANs), doc. IEEE 802.15-06-0055-21-003c, Jan. 2006

국문요약

표준 CMOS공정에서 제작된 Schottky Barrier Diode 기반의 60GHz 무선통신을 위한 주파수 하향 변환기

간단하고 가격이 낮은 60GHz 무선 통신을 위해 self-heterodyne 시스템과 ASK 시스템을 제안한다. 이 시스템은 square-law 하향 주파수 변환기를 필요로 하며, 국부 발진기 성능 열화에 강한 장점을 갖고 있다. 이러한 시스템을 구현하기 위해 0.18 μm CMOS 공정에서 250GHz의 차단 주파수를 갖는 Schottky barrier diode를 기반으로 한 60GHz square-law 하향 주파수 변환기를 개발하였다. 제작된 하향 주파수 변환기는 입력 RF와 LO의 파워가 -3dBm 일 때 23.7dB의 최소 conversion loss 를 가졌다. 제작된 주파수 변환기를 이용하여 60GHz self-heterodyne 시스템과 ASK 시스템에서의 622Mb/s 데이터 전송을 실시하였다. Self-heterodyne 시스템에서 비트 오류율은 24dB 전송 손실 상에서 10^{-10} 을 얻었다. ASK 시스템에서는 22dB 전송 손실 상에서 10^{-10} 의 비트 오류율을 얻었다.